Global Journal of Engineering and Technology [GJET].
ISSN: **2583-3359** (Online)
Frequency: Monthly
Published By GSAR Publishers
Journal Homepage Link- https://gsarpublishers.com/journal-gjet-home/

Modelling slip distribution of Chirpan-Plovdiv seismic doublet (1928), related to the heterogeneity of the earth crust derived by gravity and magnetic measurements

By

Emil Oynakov[1], Irena Alexandrova[1,] Boyko Ranguelov[2], Mariya Popova[1]

[1]Department of Seismology and Seismic Engineering in National Institute of Geophysics, Geodesy and Geography Bulgarian Academy of Sciences (NIGGG-BAS), Sofia 1113, Bulgaria
[2]Space Research and Technology Institute - Bulgarian Academy of Sciences, Sofia 1113,

[1]**https://orcid.org/0000-0001-2345-6789**
[1]**https://orcid.org/0000-0001-7207-3565**
[2]**https://orcid.org/0000-0003-2039-365X**
[1]**https://orcid.org /0009-0008-4221-971X**

Article History

Received: 25/05/2026
Accepted: 03/06/2026
Published: 05/06/2026

Vol – 5 Issue – 6

PP: - 01-07

DOI:10.5281/zenodo.20577351

Abstract

The April 1928 seismic sequence in the Maritsa River valley of southern Bulgaria, comprising the Chirpan (Mw 6.9) and Plovdiv (Mw 7.1) earthquakes, represents one of the most destructive events in southeastern Europe. Previous studies have constrained the overall fault geometry and kinematics using macroseismic data and geodetic measurements; however, the internal heterogeneity of the rupture remains poorly resolved. Contemporary models indicate that seismic rupture is an inherently heterogeneous process, characterized by localized zones of intense slip (asperities) that influence rupture propagation and energy release. Probabilistic slip models enable the reconstruction of such historical events under conditions of limited data and can be integrated with geological and geophysical information. Gravity and magnetic anomaly data from the Chirpan–Plovdiv region reveal significant lateral heterogeneity in the Earth's crust, which likely governs the development and termination of rupture processes.

Keywords: *earthquake, Bouguer gravity, magnetic anomalies, SLIP rupture.*

1. Introduction

The April 1928 earthquake sequence in the Maritsa River valley, southern Bulgaria, comprising the Chirpan event of 14 April (Mw = 6.9) and the Plovdiv event of 18 April (Mw = 7.1) (Christoskov L., et al., 1978; Ambraseys, N., 2001), represents one of the most destructive seismic episodes in southeastern Europe that time. The crustal thickness in the region reaches approximately 30–40 km. (Christoskov, L., 1998). Previous studies have constrained the overall rupture geometry and kinematics using macroseismic observations, surface faulting, and classical geodetic measurements (DIPOZE, 1931; Mirkov M., 1932, Kirov, K., 1935; Jankow K., 1945), leading to several alternative fault models and focal mechanisms (Van Eck, T., & Stoyanov, T., 1996; Dimitrov, D., et al., 2006).

While these studies provide robust constraints on large-scale deformation, the internal heterogeneity of rupture remains poorly constrained. Modern earthquake studies demonstrate that rupture is inherently heterogeneous, characterized by localized dynamic slip patches (asperities) embedded within broader regions of lower slip. Such heterogeneity plays a critical role in seismic moment release, rupture propagation, and near-field ground deformation.

In recent decades, probabilistic representations of fault slip have been widely used to model rupture processes while honoring seismic moment and fault dimensions. These approaches are particularly suitable for historical earthquakes with limited observations.

Importantly, slip models can be integrated with geological and geophysical data to assess which rupture scenarios are most consistent with the crustal structure. As early as 1984, an extended study (Ranguelov B. et al., 1984) of surface residual deformations measured by geodetic methods suggested the barrier arrest of seismic dislocations due to heterogeneities in the Earth's crust. In accordance with the adopted model, several new parameters were determined for the first time—namely stress drop, rupture energy, and the radius of the seismic source. Confirmation was sought in the spatial distribution of the aftershock sequence.

*Corresponding Author: Emil Oynakov

The Chirpan–Plovdiv region exhibits pronounced lateral heterogeneity in crustal properties, as evidenced by Bouguer gravity anomalies, magnetic anomalies, and their spatial gradients (D. Dimitrov et al. 2015; D. Dimitrov, 2024). These datasets provide insight into density and magnetic susceptibility contrasts associated with fault-bounded sedimentary basins. Although gravity and magnetic data do not directly constrain coseismic slip, they provide valuable information on crustal structure that may influence rupture propagation and termination.

2. Data and Methods

2.1. Seismotectonic setting and source parameters

The 1928 Chirpan–Plovdiv earthquake sequence occurred within the Maritsa basin, a region characterized by active extensional tectonics and fault segmentation. The sequence includes two major events: the Chirpan–Parvomay earthquake on 14 April (42.2°N, 25.3°E; depth ~9 km; Mw = 6.9) and the Popovitsa–Belozem earthquake on 18 April (42.2°N, 25.05°E; depth ~16 km; Mw = 7.1) (Christoskov L., et al., 1978, 1998; Ambraseys, N., 2001).

In this study, fault dimensions, depths, and seismic moments are adopted from previously published geodetic and seismological models (D. Dimitrov and J. Ruegg, 1996; Dimitrov D. et al., 1998). The Chirpan event is represented by a fault approximately 38 km long and ~15 km wide, whereas the 18 April event is modeled by a longer fault (~53 km) with a comparable width. These parameters are consistent with elastic dislocation modeling of geodetic profiles and seismic moment estimates. The results of the stress transfer in the earthquake zone are also reported (Papadimitriou E., V. Karakostas, M. Tranos, B. Ranguelov, D. Gospodinov., 2007)

2.2. Slip modeling

To explore the range of rupture heterogeneity, we employ a probabilistic approach in which slip distributions are generated as spatially correlated random fields defined on rectangular fault planes. The models are constrained to reproduce the prescribed seismic moment, fault dimensions, and average slip.

Slip distributions are generated using the SLIPREAL algorithm, which constructs two-dimensional slip fields with predefined spectral decay properties and correlation lengths along strike and down dip. The resulting slip distributions are smoothly tapered toward the fault edges, ensuring physically realistic rupture models. Multiple realizations are produced by varying the random seed while keeping source parameters fixed, thereby sampling the ensemble of statistically admissible rupture scenarios.

Slip amplitudes are expressed in centimeters, with mean values of approximately ~1 m for the 14 April event and ~1.5 m for the 18 April event, consistent with their seismic moments . These probabilistic models are not intended to reproduce a unique rupture history but rather to provide a statistically consistent representation of slip heterogeneity constrained by the available data (fixed seismic moment, fault geometry, and general slip distribution characteristics).

2.3. Geodetic constraints

Geodetic observations consist primarily of classical leveling profiles measured before and after the earthquakes (Мирков M. 1932, Jankow K., 1945). Previous studies interpreted these data using elastic dislocation theory to derive fault geometry, depth, and average slip (Dimitrov, D., et al., 2020; Dimitrov, D. S., et al., 2006).

In this study, published fault models are used as independent constraints on rupture geometry. Rather than re-inverting the geodetic data, these models guide the selection of fault dimensions and ensure consistency between simulated rupture scenarios and observed surface deformation patterns.

2.4. Gravity and magnetic data

The dataset includes high-resolution gravity and magnetic measurements acquired at 193 gravity stations and 180 magnetic stations in the study area (D. Dimitrov et al., 2015).

The crustal structure is investigated using Bouguer gravity anomalies (Fig. 1) and total magnetic anomalies (Fig. 3). Vertical gradients of both fields (Figs. 2 and 4) are computed to enhance short-wavelength features and highlight lateral contrasts associated with fault zones and structural boundaries.

Spatial correlation between gravity and magnetic anomalies (Fig. 5) is also analyzed to identify regions of coupled or decoupled density and magnetic contrasts. Zones of low or negative correlation are interpreted as structurally complex regions or transitions between crustal blocks. To improve the accuracy of the interpretation, the density and magnetic properties of representative rock types from the study area were determined under both laboratory and field conditions following paleoseismic trenching in the region (Vanneste K. et al., 2006).

Although gravity and magnetic data do not directly constrain coseismic slip, they provide independent information on inherited crustal heterogeneity that may influence rupture segmentation and propagation.

3. Results and discussion

3.1. Bouguer gravity anomaly field

The Bouguer gravity anomaly map (Fig. 1) reveals pronounced lateral variations in crustal density. Broad negative anomalies dominate the Maritsa basin, while higher gravity values to the north and south reflect denser basement blocks

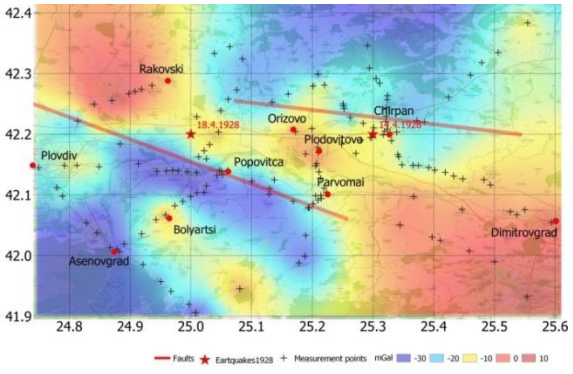

*Corresponding Author: Emil Oynakov

Fig.1 Gravity (Bouguer-mGal) anomalies in the studied area and leveling benchmarks on which gravity measurements were carried out

The epicentral regions and rupture zones are located within transitional areas between contrasting gravity anomalies.

3.2. Vertical gradient of Bouguer gravity

The vertical gradient field (Fig. 2) highlights linear zones of high gradient amplitude, trending predominantly E–W to NE–SW. These features delineate sharp lateral density contrasts and likely correspond to fault zones or block boundaries.

Some gradient maxima spatially coincide with modeled rupture segments, and rupture terminations are associated with areas where gradient amplitude decreases or changes orientation, suggesting fault segmentation.

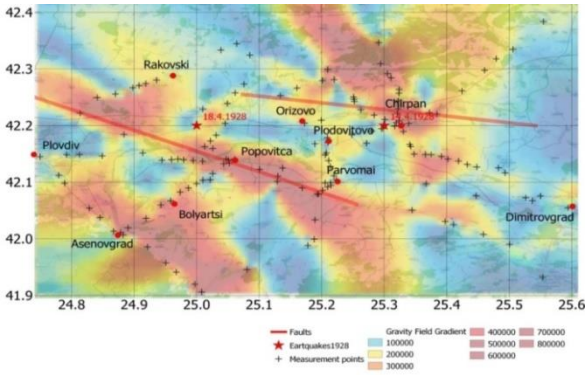

Fig.2. Vertical gradient of the Bouguer anomaly in the study area

3.3. Magnetic anomaly field

The magnetic anomaly field (Fig. 3) exhibits higher spatial variability compared to gravity, with sharp short-wavelength contrasts reflecting heterogeneity in both basement and sedimentary cover.

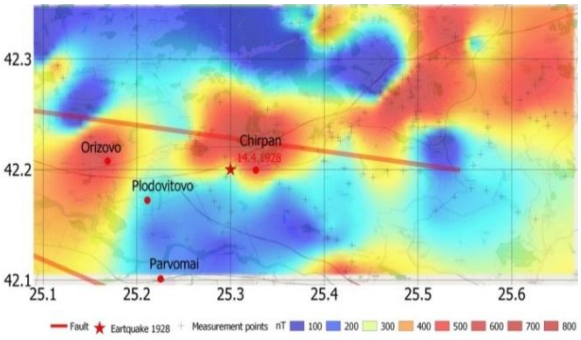

Fig. 3 Magnetic anomalies (total vector-nT) in and near the Chirpan Fault

The rupture zone of the 14 April event crosses regions characterized by moderate to strong magnetic gradients rather than extreme anomaly values.

3.4. Vertical gradient of magnetic anomalies

The vertical gradient of the magnetic field (Fig. 4) emphasizes shallow structures. Several linear anomalies coincide with known faults, including segments of the Chirpan–Orizovo–Plodovitovo fault system.

In some areas, gravity and magnetic gradient maxima overlap, indicating major crustal discontinuities expressed in both density and magnetic susceptibility.

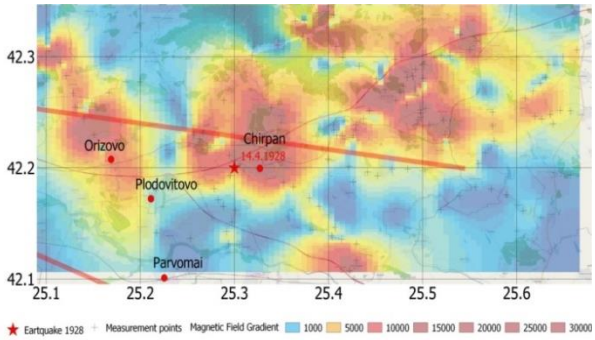

Fig.4 Vertical gradient of magnetic anomalies in the area of the April 14, 1928 earthquake.

3.5. Correlation between gravity and magnetic fields

The spatial distribution of the correlation coefficient (Fig. 5) reveals alternating zones of high positive and low or negative correlation, indicating variable relationships between density and magnetic sources. The rupture zones are located within or adjacent to regions of low correlation, suggesting structurally complex crustal domains.

3.6. Probabilistic rupture for the Chirpan earthquake

Representative slip realizations (Fig. 6) show heterogeneous slip distributions ranging from near-zero values at fault edges to maximum values of ~250 cm, with peak slip reaching ~300 cm (Fig. 8).

Slip is concentrated at intermediate depths (~2–9 km), while shallow and deep portions exhibit lower amplitudes. A dominant central asperity is consistently observed across realizations.

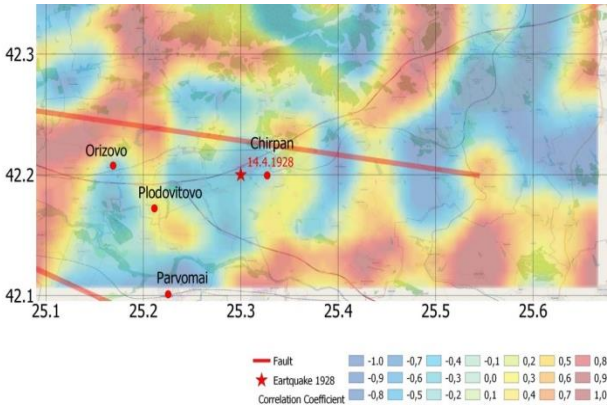

Fig.5. Correlation between Bouguer gravity and magnetic anomalies

*Corresponding Author: Emil Oynakov

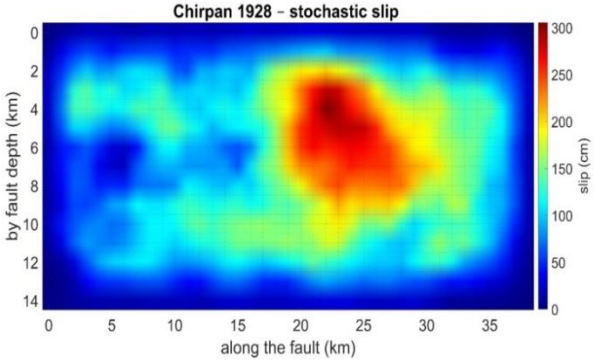

Fig.6 Slip rupture along the Chirpan Fault

3.7. Probabilistic rupture for the Plovdiv earthquake

Slip models (Fig. 7) exhibit a larger rupture area and higher overall slip amplitudes, consistent with the larger seismic moment. Maximum slip reaches ~275 cm and up to ~300 cm (Fig. 8).

Multiple elongated asperities are observed along strike, indicating greater spatial variability compared to the Chirpan event.

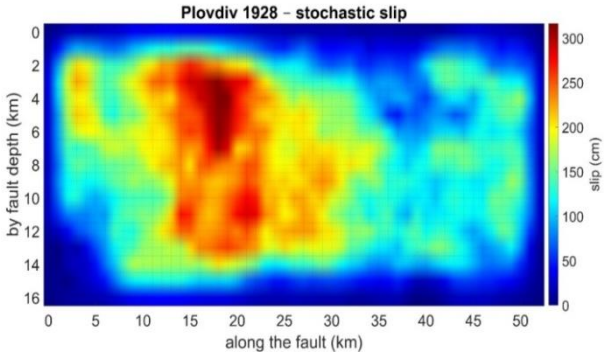

Fig.7. Slip rupture along the Popovitca fault

3.8. Slip profiles

Slip profiles along strike and depth (Fig. 8) reveal systematic characteristics common to both earthquakes, with peak slip consistently located at intermediate depths and decreasing toward the rupture boundaries.

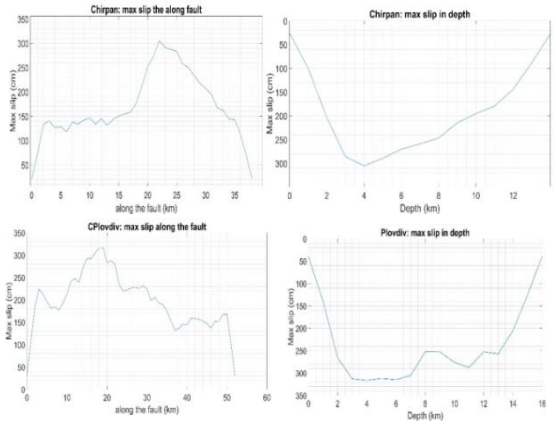

Fig.8. Probabilistic characteristics of slippage for both events

3.9. Contemporary seismicity

The spatial and depth distribution of instrumental seismicity for the period from 1991 to 2025 (Fig. 9) outlines zones of persistent seismic activity that broadly coincide with gravity and magnetic gradient lineaments and with the 1928 rupture zones (Solakov D. et al., 2020; as well as data from the Bulgaria Digital Seismic Network – doi.org/10.7914/SN/BS).

Although not directly linked to the 1928 events, this seismicity highlights crustal structures controlling ongoing deformation.

a)

b)

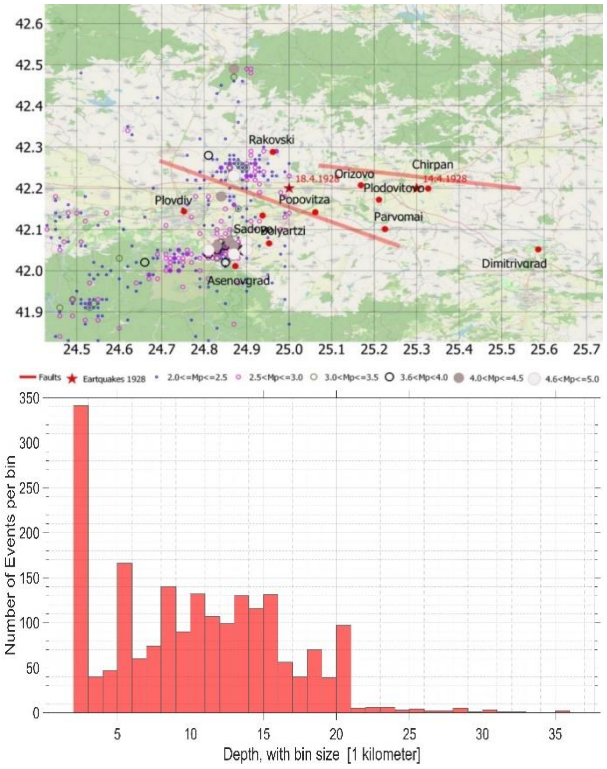

Fig. 9. Spatial (a) and depth (b) distribution of modern instrumental seismicity in the area.

This study demonstrates that probabilistic slip modeling, when constrained by independently derived source parameters and combined with geophysical datasets, provides a robust framework for reconstructing physically plausible rupture scenarios for historical earthquakes (1,2,3).

The results highlight that both the Chirpan (14 April 1928) and Plovdiv (18 April 1928) earthquakes are characterized by pronounced slip heterogeneity, with systematically developed asperities located at intermediate depths (approximately 2–9 km). Despite differences in rupture dimensions and seismic moment, both events exhibit consistent structural patterns, including reduced slip toward the fault edges and concentration of slip within the central portions of the rupture planes (Figs. 6–8).

The heterogeneity of the Earth's crust plays an important role in controlling the complexity of ruptures (Wesnousky, S. G. (2006); Das, S., & Aki, K. (1977); Aochi, H., & Fukuyama, E.

*Corresponding Author: Emil Oynakov

(2002); Manighetti, I., et al. (2015)). A key outcome of this work is the identification of a systematic spatial relationship between dynamic slip regions and crustal heterogeneity derived from gravity and magnetic data. Dynamic slippatches (>150–200 cm) preferentially coincide with zones of elevated gravity gradient amplitude (Fig. 2) and, in several cases, with corresponding magnetic gradient anomalies (Fig. 4). These zones represent sharp lateral contrasts in physical properties and are interpreted as major structural boundaries or fault-controlled transitions within the crust.

Conversely, rupture propagation through regions characterized by low gradient amplitudes or reduced correlation between gravity and magnetic fields (Fig. 5) is associated with diminished slip. This observation suggests that such regions act either as barriers to rupture propagation or as zones of distributed deformation where slip is less efficiently localized.

The correlation analysis further indicates that rupture zones are frequently located within or adjacent to areas of low or negative gravity–magnetic correlation, reflecting structurally complex domains where density and magnetic susceptibility contrasts are decoupled. These domains likely correspond to heterogeneous lithological assemblages or transitional zones between crustal blocks, which may play a significant role in controlling rupture segmentation.

4. Conclusions

The rupture amplitudes obtained for the two events considered in the present study are consistent with the empirical scaling relationships between seismic moment (Mo), rupture area and average displacement, which provides confidence in the physical plausibility of the modeled rupture fields (Leonard, M. (2010); Blaser, L., et al. (2010)).

The comparison between the two events reveals that the larger Plovdiv earthquake exhibits more spatially distributed and elongated asperities along strike (Fig. 7), whereas the Chirpan event is dominated by a more compact central asperity (Fig. 6). This difference is consistent with the increased rupture length and complexity of the second event and suggests a stronger influence of fault segmentation and structural variability.

Importantly, the probabilistic models do not aim to reproduce a unique rupture history but instead provide a statistical ensemble of admissible slip distributions consistent with available constraints, including seismic moment, fault geometry, and average slip. Within this framework, the observed consistency of key features across multiple realizations increases confidence in the inferred structural controls on rupture.

The integration of geodetic constraints, probabilistic slip modeling, and potential field data demonstrates that inherited crustal heterogeneity exerts a first-order control on rupture localization, slip amplitude distribution, and segmentation (Somerville, P. G., et al. (1999); Mai, P. M., et al. (2005); Manighetti, I. et al. (2007)). This finding has important implications for seismic hazard assessment, as it suggests that spatial variations in crustal properties must be explicitly considered when evaluating potential rupture scenarios. The geodynamic interpretation of all observations, supports the conclusion suggested by most of the researchers, that this couple events are realized in extensional geodynamics with N-S extension direction, thus providing almost clear normal faulting bor both strong seismic events.

Finally, the methodological approach presented here is broadly applicable to other historical earthquakes lacking detailed instrumental data (for example, the Sofia Basin). By combining stochastic rupture modeling with independent geophysical constraints, it is possible to derive physically meaningful, statistically and geodynamic robust interpretations of earthquake processes, even in data-limited environments.

Acknowledgments

The presented work was performed within the project Assessment of Earthquake Ground Motion Amplification in the Sofia Basin, funded by the Bulgarian National Science Fund, contract number КП-06-Н64/1 from 15.12.2022.

REFERENCES

1. Christoskov L., D.Sokerova, S.Rijikova, 1978. Catalogue of the Historical Earthquakes in Bulgaria. Funds of the Geophysical Institute, Bulgarian Academy of Sciences
2. Christoskov, L. (1998). 70 years since the 1928 Chirpan–Plovdiv earthquakes. In *Proceedings of the Symposium "Geodynamic Studies Related to the 1928 Chirpan–Plovdiv Earthquakes"* (pp. 5–21), Sofia, October 1998.
3. Ambraseys, N. N. (2001). The Kresna earthquake of 1904 in Bulgaria. *Annals of Geophysics*, *44*(1).
4. Direction for Support and Reconstruction of the Area Damaged by the 1928 Earthquakes (DIPOZE) (1931), Report on the Activities Undertaken From April 25, 1928 Until November 1, 1931 (in Bulgarian), 421 pp., State Press, Sofia.
5. Mirkov M. (1932) Precision levelling measurements in the seismogenic zone of southern Bulgaria, Bull. Inst. Nat. Geogr., pp. 34-39, Sofia. (in Bulgarian).
6. Kirov K, "Contribution to the description of the earthquakes of April 14 and 18, 1928 in southern Bulgaria", Collection of the Bulgarian Academy of Sciences, vol. XXIX, p., 116 p. (1935)
7. Jankow K., 1945. Terrain changes caused by the earthquakes of 14 and 18 April 1928 in South Bulgaria. In "Earthquakes in Bulgaria" N29-31/1928-1930, Sofiq, 131-136 (in Bulgarian)
8. Christoskov, L. (2000), Energy and source parameters of the strong Bulgarian earthquakes after 1900, Rep. Geod. 3(48), pp. 15 – 20, Warsaw Univ. of Technol., Warsaw
9. Dimitrov, D., Ruegg, J. C., Meyer, B., Chabalier, J. B., Botev, E., & Briole, P. (2020). The 1928 Plovdiv sequence: Fault model constrained from

*Corresponding Author: Emil Oynakov

geodetic data and surface breaks. *Proceedings SES 2020*, 250-261.

10. Dimitrov, D. S., De Chabalier, J. B., Ruegg, J. C., & Botev, E. (2006). The 14 and 18 April 1928 Chirpan-Plovdiv Earthquakes–fault model from geodetic and seismic data. GEOSCIENCES 2006.
11. Ranguelov B., S. Rizikova, B. Dimitrov., Residual Deformations of the 1928 Plovdiv's Earthquakes and Determination of New Parameters., Geol. Balcanica, 14.5.1984, pp. 67-72.
12. Д. Димитров, Е. Ботев, В. Протопопова, М. Еверхард, Е. Михайлов и Ил. Чолаков (2015) "Геофизични аномалии в Горнотракийската низина и връзката им с главните разломи, активирали се при земетресенията от април 1928 г. и съвременната инструментална сеизмичност" S1-01, Доклади от Седма национална конференция по геофизика с международно участие „Геофизика 2015", 25 години ДГБ, 20 – 23 май 2015 г., София.
13. M. Everaerts, D. Dimitrov, I. Cholakov, Th. Camelbeeck. Gravity and magnetic measurements in the area Chiran – Plovdiv (Bulgaria). EGU 2006
14. Van Eck, T., & Stoyanov, T. (1996). Seismotectonics and seismic hazard modelling for Southern Bulgaria. *Tectonophysics*, *262*(1-4), 77-100.
15. Димитров Д., Ботев Е., Протопопова В., Еверхард М., Михайлов Е., Чолаков Ил., Георгиев Ив.. Геофизични аномалии в Горнотракийската низина и връзката им с главните разломи от земетресенията през април 1928 г. и съвременната инструментална сеизмичност. 7-ма Национална конференция по геофизика с международно участие „Геофизика 2015", 20-22 май 2015, София,, CD S1-O2, 2015, ISBN:1314-2518.
16. Dimitrov, d. S. (2024). Earthquakes chirpan-plovdiv of april 1928 - mechanism, nature, seismic cycle and hazard. Ses 2024 twentieth anniversary international scientific conference, space, ecology, safety 22 – 25 october 2024, sofia, bulgaria, pp. 217-223
17. DIMITROV, D., & RUEGG, J. (1996). Results of a Geodetic Study Concerning Seismotectonics Parameters of the 1928 Earthquakes in South Bulgaria. *Bulgarian Geophysical Journal: Bulgarian Academy of Sciences*, 63-72.
18. Dimitrov, D., et al. (1998). Analysis of seismotectonic deformations associated with the April 1928 Plovdiv earthquakes. In *Proceedings of the Symposium "Geodynamic Studies Related to the 1928 Chirpan–Plovdiv Earthquakes"* (pp. 177–180), Sofia, October 1998.
19. Papadimitriou E., V. Karakostas, M. Tranos, B. Ranguelov, D. Gospodinov., 2007. Static stress changes associated with normal faulting earthquakes in South Balkan area., Int. J. Earth Sci. (Geol. Rundsch.), Springer-Verlag, No 96, pp.911-924
20. Vanneste K, Radulov A, DeMartini P, Nikolov G, Petermans T, Verbeeck K, Camelbeeck T, Pantosti D, Dimitrov D,p Shanov S (2006) Paleoseismologic investigation of the fault rupture of the 14 April 1928 Chirpan earthquake (M6.8) Southern Bulgaria. J Geophys Res 111 B01303. DOI10.1029/2005JB003814
21. Bonchev, S., and P. Bakalov (1928), Les tremblements de terre dans la Bulgarie du Sud les 14 et 18 avril 1928, Rev. Bulg. Geol. Soc., 1(2), 51 – 63
22. Mai, P. M., & Beroza, G. C. (2002). A spatial random field model to characterize complexity in earthquake slip. Journal of Geophysical Research: Solid Earth, 107(B11) DOI: 10.1029/2001JB000588
23. Herrero, A., & Bernard, P. (1994). A kinematic self-similar rupture process for earthquakes. Bulletin of the Seismological Society of America, 84(4), 1216-1228.
24. Lavallée, D., Liu, P., & Archuleta, R. J. (2006). Stochastic model of heterogeneity in earthquake slip spatial distributions. Geophysical Journal International, 165(2), 622-640.
25. Wesnousky, S. G. (2006). Predicting the endpoints of earthquake ruptures. Nature, 444(7117), 358-360.
26. Santosh K. Das & Keiiti Aki (1977). A numerical study of two-dimensional spontaneous rupture propagation. Journal of Geophysical Research, 82(36), 5658–5670. https://doi.org/10.1029/JB082i036p05658
27. Hiroyuki Aochi & Eiichi Fukuyama (2002). Three-dimensional nonplanar simulation of the dynamic rupture process. Geophysical Research Letters, 29(13), 1614. https://doi.org/10.1029/2002GL015123
28. Isabelle Manighetti, Clément Perrin, Jean-Paul Ampuero, Frédéric Cappa & Yves Gaudemer (2015) Location of largest earthquake slip and fast rupture controlled by along-strike change in fault structural maturity due to fault growth. Journal of Geophysical Research: Solid Earth. https://doi.org/10.1002/2015JB012671
29. Wells, D. L., & Coppersmith, K. J. (1994). New empirical relationships among magnitude, rupture length, rupture width, rupture area, and surface displacement. Bulletin of the seismological Society of America, 84(4), 974-1002.
30. Leonard, M. (2010). Earthquake fault scaling: Self-consistent relating of rupture length, width, average displacement, and moment release. Bulletin of the Seismological Society of America, 100(5A), 1971-1988.
31. Blaser, L., Krüger, F., Ohrnberger, M., & Scherbaum, F. (2010). Scaling relations of

*Corresponding Author: Emil Oynakov

earthquake source parameter estimates with special focus on subduction environment. Bulletin of the Seismological Society of America, 100(6), 2914-2926.

32. Paul G. Somerville et al. (1999). Characterizing crustal earthquake slip models for the prediction of strong ground motion. Seismological Research Letters, 70(1), 59–80 https://doi.org/10.1785/gssrl.70.1.59
33. Mai, P. M., Spudich, P., & Boatwright, J. (2005). Hypocenter locations in finite-source rupture models. Bulletin of the Seismological Society of America, 95(3), 965-980.
34. Manighetti, I., Campillo, M., Bouley, S., & Cotton, F. (2007). Earthquake scaling, fault segmentation, and structural maturity. Earth and Planetary Science Letters, 253(3-4), 429-438.
35. Mai, P. M., & Beroza, G. C. (2002). A spatial random field model to characterize complexity in earthquake slip. *Journal of Geophysical Research: Solid Earth*, 107(B11), ESE 10-1–ESE 10-21.
36. Herrero, A., & Bernard, P. (1994). A kinematic self-similar rupture process for earthquakes. *Bulletin of the Seismological Society of America*, 84(4), 1216–1228.
37. Lavallée, D., Liu, P., & Archuleta, R. J. (2006). Stochastic model of heterogeneity in earthquake slip spatial distributions. *Geophysical Journal International*, 165(2), 622–640.
38. Leonard, M. (2010). Earthquake fault scaling: Self-consistent relating of rupture length, width, average displacement, and moment release. *Bulletin of the Seismological Society of America*, 100(5A), 1971–1988.
39. Blaser, L., Krüger, F., Ohrnberger, M., & Scherbaum, F. (2010). Scaling relations of earthquake source parameters and their variability for different rupture mechanisms and tectonic regimes. *Bulletin of the Seismological Society of America*, 100(6), 2916–2930.
40. Wesnousky, S. G. (2006). Predicting the endpoints of earthquake ruptures. *Nature*, *444*(7117), 358-360.
41. Das, S., & Aki, K. (1977). Fault plane with barriers: A versatile earthquake model. *Journal of Geophysical Research*, 82(36), 5658–5670.
42. Aochi, H., & Fukuyama, E. (2002). Three-dimensional nonplanar simulation of the 1992 Landers earthquake. *Journal of Geophysical Research: Solid Earth*, 107(B2), ESE 3-1–ESE 3-14.
43. Manighetti, I., Schmittbuhl, J., & Marsan, D. (2015). Slip accumulation and fault roughness: Insights into earthquake scaling. *Journal of Geophysical Research: Solid Earth*, 120(6), 4161–4177.
44. Somerville, P. G., Irikura, K., Graves, R. W., Sawada, S., Wald, D. J., Abrahamson, N. A., Iwasaki, Y., Kagawa, T., Smith, N. F., & Kowada, A. (1999). Characterizing crustal earthquake slip models for the prediction of strong ground motion. *Seismological Research Letters*, 70(1), 59–80.
45. Mai, P. M., Spudich, P., & Boatwright, J. (2005). Hypocenter locations in finite-source rupture models. *Bulletin of the Seismological Society of America*, 95(3), 965–980.
46. Manighetti, I., Campillo, M., Bouley, S., & Cotton, F. (2007). Earthquake scaling, fault segmentation, and structural maturity. *Earth and Planetary Science Letters*, 253(3–4)

*Corresponding Author: Emil Oynakov